Aromatase Imaging with [*N*-Methyl-^{11}C]Vorozole PET in Healthy Men and Women

Anat Biegon[1,2], David L. Alexoff[2], Sung Won Kim[3], Jean Logan[4], Deborah Pareto[5], David Schlyer[2], Gene-Jack Wang[3], and Joanna S. Fowler[2,6]

[1]Stony Brook University School of Medicine, Stony Brook, New York; [2]Brookhaven National Laboratory, Upton, New York; [3]National Institute on Alcoholism and Alcohol Abuse, Bethesda, Maryland; [4]New York University Langone Medical Center, New York, New York; [5]Institut de Recerca Hospital Universitari Vall d'Hebron, Universitat Autònoma de Barcelona, Alta Tecnologia, Barcelona, Spain; and [6]State University of New York at Stony Brook, Stony Brook, New York

Aromatase, the last and obligatory enzyme catalyzing estrogen biosynthesis from androgenic precursors, can be labeled in vivo with ^{11}C-vorozole. Aromatase inhibitors are widely used in breast cancer and other endocrine conditions. The present study aimed to provide baseline information defining aromatase distribution in healthy men and women, against which its perturbation in pathologic situations can be studied. **Methods:** ^{11}C-vorozole (111–296 MBq/subject) was injected intravenously in 13 men and 20 women (age range, 23–67 y). PET data were acquired over a 90-min period. Each subject had 4 scans, 2 per day separated by 2–6 wk, including brain and torso or pelvis scans. Young women were scanned at 2 discrete phases of the menstrual cycle (midcycle and late luteal). Men and postmenopausal women were also scanned after pretreatment with a clinical dose of the aromatase inhibitor letrozole. Time–activity curves were obtained, and standardized uptake values (SUV) were calculated for major organs including brain, heart, lungs, liver, kidneys, spleen, muscle, bone, and male and female reproductive organs (penis, testes, uterus, ovaries). Organ and whole-body radiation exposures were calculated using OLINDA software. **Results:** Liver uptake was higher than uptake in any other organ but was not blocked by pretreatment with letrozole. Mean SUVs were higher in men than in women, and brain uptake was blocked by letrozole. Male brain SUVs were also higher than SUVs in any other organ (ranging from 0.48 ± 0.05 in lungs to 1.5 ± 0.13 in kidneys). Mean ovarian SUVs (3.08 ± 0.7) were comparable to brain levels and higher than in any other organ. Furthermore, ovarian SUVs in young women around the time of ovulation (midcycle) were significantly higher than those measured in the late luteal phase, whereas aging and cigarette smoking reduced ^{11}C-vorozole uptake. **Conclusion:** PET with ^{11}C-vorozole is useful for assessing physiologic changes in estrogen synthesis capacity in the human body. Baseline levels in breasts, lungs, and bones are low, supporting further investigation of this tracer as a new tool for detection of aromatase-overexpressing primary tumors or metastases in these organs and optimization of treatment in cancer and other disorders in which aromatase inhibitors are useful.

Key Words: vorozole; aromatase inhibitors; PET; biodistribution; dosimetry

J Nucl Med 2015; 56:580–585
DOI: 10.2967/jnumed.114.150383

Aromatase, a member of the cytochrome P450 protein superfamily (*1*), is a unique product of the CYP19a gene. Aromatase regulates the last step of estrogen biosynthesis, aromatizing the A ring of androgens such as androstenedione and testosterone to estrone and estradiol, respectively. Aromatase is expressed in various peripheral organs as well as in the brain of rodents, nonhuman primates, and humans (*2–5*). To date, there have been no published studies of aromatase distribution throughout the human body or its regulation by sex and hormonal status, although animal studies suggest that brain aromatase activity is higher in males than in females and is modulated by changes in testosterone levels but not in the phase of the female estrus cycle (*3,6,7*).

Brain aromatase, along with specific estrogen receptors, has been implicated in cellular proliferation, reproduction, sexual behavior, aggression, cognition, memory, and neuroprotection in various animal species (*8,9*). Increases in aromatase expression are also implicated in a wide range of human diseases, most prominently in breast cancer (*10*), but also other pathologies including endometriosis (*11*), lung cancer (*12*), and hepatic cancer (*13*).

Several aromatase inhibitors, including vorozole ((*S*)-6-[(4-chlorophenyl)(1H-1,2,4-triazol-1-yl)methyl]-1-methyl-1H-benzotriazole) (inhibition constant, 0.7 nM) (Fig. 1), letrozole, and cetrozole have been labeled with ^{11}C using ^{11}C-methyl iodide and evaluated as radiotracers for in vivo imaging of brain aromatase in rodents and primates (*14–20*). ^{11}C-vorozole brain scans revealed high specific binding in the rhesus and baboon amygdala, similar to results obtained with autoradiography of the rat brain (*16,17,19*). We have recently reinvestigated and modified the radiosynthesis and purification of ^{11}C-vorozole (*19*). The pure ^{11}C-vorozole was tested and validated in the brains of female baboons and was the first aromatase radiotracer used in human brain studies (*4*).

Despite the importance of aromatase in physiologic and pathologic processes and the increasing use of aromatase inhibitors, there are no published quantitative, noninvasive studies of the distribution and regulation of aromatase in living humans. We hereby show that ^{11}C-vorozole is a useful ligand for studies of aromatase in the human body.

MATERIALS AND METHODS

Subjects and Study Design

Thirty-three healthy subjects, 13 men and 20 women (10 premenopausal and 10 postmenopausal), were enrolled in the study, which was approved by the Institutional Review Board and the Radioactive Drug

Received Oct. 24, 2014; revision accepted Jan. 19, 2015.
For correspondence or reprints contact: Anat Biegon, Department of Neurology, Stony Brook University, Stony Brook, NY 11794-2565.
E-mail: anat.biegon@stonybrook.edu
Published online Feb. 19, 2015.
COPYRIGHT © 2015 by the Society of Nuclear Medicine and Molecular Imaging, Inc.

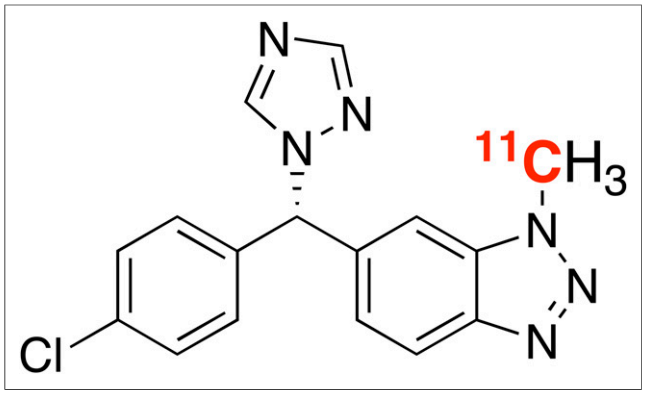

FIGURE 1. Structure of *N*-methyl-^{11}C-vorozole highlighting position of ^{11}C.

Research Committee of Stony Brook University/Brookhaven National Laboratory. All subjects gave written informed consent. The study inclusion criteria were age 21–70 y, good health, and ability to give informed consent. Subjects were excluded for recent or current use of steroids (including contraceptives), recreational drugs, and medications affecting brain function; a history of neurologic, psychiatric, or metabolic disorders; and pregnancy.

The study protocol entailed 2 visits and 4 scans per subject, including combinations of brain, body, retest, and blocking studies. To obtain images of all major body organs, the subjects were positioned in the PET scanner with the head, torso, or pelvis in the center of the camera field of view. Blocking studies were performed on men and postmenopausal women 2 h after an oral dose (2.5 mg) of letrozole (Femara; Novartis (*15*)). During the screening visit, premenopausal women were asked to report the date of their last menstrual period and their PET studies were scheduled to coincide with the nearest midcycle, when plasma estrogen levels are at their highest, or during the late luteal/early follicular phase, when estrogen levels are lower. Blood samples were taken from all subjects on the day of the PET study, and plasma hormone levels were measured by a commercial laboratory (Quest). Total testosterone and estradiol were measured in all subjects. Samples from women were additionally analyzed for progesterone and luteinizing hormone. Plasma from subjects who responded positively to the question "do you smoke cigarettes" was analyzed for nicotine and its major metabolite, cotinine.

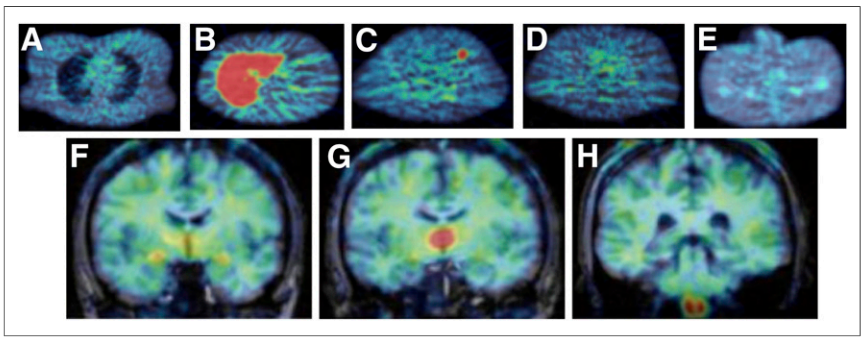

FIGURE 2. ^{11}C-vorozole uptake in human body. Pseudocolored (rainbow spectrum) examples of ^{11}C-vorozole uptake in body and brain are shown. For anatomic verification, peripheral organ axial images (A–E) were overlaid on the attenuation scan obtained immediately before the emission scan. Brain coronal images (F–H) were coregistered and overlaid on brain MR images obtained separately. A = female, level of breasts and lungs; B = female, level of liver; C = female at midcycle, level of ovary; D = female, level of lower pelvis; E = male, level of lower pelvis; F = level of amygdala; G = level of thalamus; H = level of medulla.

PET Data Acquisition and Analysis

Pure ^{11}C-vorozole was synthesized and purified as previously described (*19*). PET images were acquired over a 90-min period using a whole-body positron emission tomograph (Siemens HR+, 4.5 × 4.5 × 4.8 mm at the center of the field of view) in 3-dimensional dynamic acquisition mode as previously described (*19*). For each PET scan, subjects received an injection of ^{11}C-vorozole (111–296 MBq; specific activity > 3.7 MBq/nmol at the time of injection). An arterial plasma input function for ^{11}C-vorozole was obtained from arterial blood samples withdrawn every 2.5 s for the first 2 min (Ole Dich automatic blood sampler) and then at 3, 4, 5, 6, 8, 10, 15, 20, 30, 45, 60, and up to 90 min (end of study). All samples were centrifuged to obtain plasma, which was counted, and selected samples were assayed for the presence of unchanged ^{11}C-vorozole.

The fraction of ^{11}C-vorozole remaining in plasma was determined by a solid-phase extraction using a laboratory robot (*21*) after validation by high-performance liquid chromatography using conditions described previously (*19*). Plasma (0.4 mL) was added to 3 mL of pH 7 phosphate buffer and applied to a previously conditioned C18 cartridge (BondElut LRC, 500 mg; Varian, Inc.), which was then washed sequentially with 3 × 5 mL of water. All wash fractions and the C18 cartridge were counted. The ratio of the radioactivity remaining on the C18 cartridge to that of the total radioactivity recovered is the percentage of unchanged tracer, after corrections for radioactive decay, background, and geometry-dependent counting efficiency (*21*). Radioactivity recovery was 90%–110%.

PET images were reconstructed using the filtered backprojection algorithm into a 128 × 128 × 63 matrix, with a voxel size of 1.72 × 1.72 × 2.43 mm. Regions of interest (ROIs) included heart, lungs, liver, kidneys, muscle, bone, and male and female reproductive organs (penis, testes, uterus, and ovary) and several brain regions (thalamus, amygdala, cerebellum, cortex, medulla, preoptic area, putamen, and cortical white matter). Brain ROIs were drawn over available brain MR images of the same subjects, coregistered to the PET study by maximizing mutual information with statistical parametric mapping (SPM8). Transmission scans were used to provide anatomic localization for torso and pelvis scans. ROIs were projected onto the dynamic images to obtain time–activity curves. Regions occurring bilaterally were averaged. ^{11}C concentration in each ROI was divided by the injected dose to obtain the percentage dose per cubic centimeter. Standardized uptake values (SUVs) were calculated from the mean values collected between the following periods: 2–90 min, 2–60 min, 30–60 min, 30–90 min, and 60–90 min.

Dosimetry was calculated using OLINDA/EXM software, version 1.1 (*22*). Urine samples were taken at the end of the PET acquisition, counted, and included in the dosimetry estimation model.

Statistical analysis was performed using Statview software (version 4.1). The effect of the scanning interval used to calculate SUV was tested by a 1-way ANOVA. Differences were considered significant if the *P* value was less than 0.05. The effects of blocking, sex, and menstrual cycle were tested by a 2-way ANOVA (treatment/subject group × ROI) followed if relevant by post hoc regional comparisons by the Fisher protected least significant difference test, with a *P* value of less than 0.05 considered significant.

RESULTS

The study population comprised healthy men and women (mean age ± SD, 42 ± 15.6 y; range, 23–67 y). These included 10 postmenopausal women (57.8 ± 4.9 y), 10 younger

women with intact menstrual cycles (28.6 ± 5.9 y), 7 younger men (27 ± 5.6 y), and 6 older men (55.4 ± 5.9 y).

The mean injected dose was 205.7 ± 47.7 MBq (range, 92.5–273.8 MBq), and the specific activity at the time of injection was 48.5 ± 21.8 MBq/nmol (range, 17.4–73.2 MBq/nmol). The elapsed time between the end of synthesis and injection was 60 min. The mean and SD of the administered mass of vorozole was 1.57 ± 0.95 μg (range, 0.7–3.2 μg). There were no adverse or clinically detectable pharmacologic effects in any of the 33 subjects. The final distribution of the studies acquired was the following: brain baseline, 33 (13 men and 20 women); brain blocking, 9 (6 men and 3 women); brain retest, 16 (5 men and 11 women); torso baseline, 9 (4 men and 3 women); torso blocking, 6 (2 men and 4 women); torso retest, 5 (2 men and 3 women); pelvis baseline, 19 (6 men and 13 women); pelvis blocking, 3 (3 men); and pelvis retest, 11 (3 men and 8 women).

As previously reported, plasma levels of the tracer declined slowly, with unchanged parent compound accounting for about 60% of the radioactivity in plasma 90 min after injection in both men and women (*4*). The tracer showed fast uptake and washout in most peripheral organs, besides the liver and the ovary at midcycle (Figs. 2 and 3). Attempts to derive kinetic parameters using the metabolite-corrected plasma input function and modeling, as used previously in the brain (*4*), were unsuccessful, probably because of the low uptake. In the brain, ^{11}C-vorozole showed a rapid uptake followed by a region-dependent washout. To facilitate a comparison of tracer uptake throughout the body, SUVs were calculated on the basis of data acquired over several intervals (2–30 min, 2–60 min, 2–90 min, and 30–60 min). There were no statistically significant differences among the 4 intervals (P = 0.68). The values reported here represent the 30- to 60-min interval, which was considered the most amenable to standard clinical application.

TABLE 1
Mean SUVs in Selected Organs of Healthy Men and Women

Organ	Men			Women		
	n	Mean	SEM	*n*	Mean	SEM
Liver	4	12.2	2.2	7	8.9	1.6
Ovary	NA	NA	NA	9	3.1	0.7
Hypothalamus	13	2.97	0.16	20	2.77	0.2
Thalamus	13	2.6	0.12	20	2.5	0.18
Preoptic area	13	1.97	0.1	20	1.75	0.07
Amygdala	13	1.92	0.1	20	1.73	0.06
Endometrium	NA	NA	NA	10	1.7	0.16
Medulla	13	1.82	0.12	20	1.6	0.1
Putamen	13	1.6	0.07	20	1.37	0.05
Kidney	4	1.5	0.13	3	1.35	0.15
White matter	13	1.44	0.07	20	1.24	0.04
Cerebellum	13	1.27	0.07	20	1.18	0.04
Bone (sacrum)	4	1.24	0.1	5	1.18	0.07
Spleen	4	1.12	0.05	4	0.95	0.1
Testes	3	1.06	0.08	NA	NA	NA
Muscle (glut)	6	0.94	0.08	13	0.95	0.04
Penis	6	0.84	0.09	NA	NA	NA
Lungs	5	0.48	0.05	3	0.45	0.04

NA = not applicable.
2-way ANOVA by organ and sex performed after exclusion of sex-specific organs revealed significant main effect of sex and organ (both $P < 0.001$) but no significant interaction term.

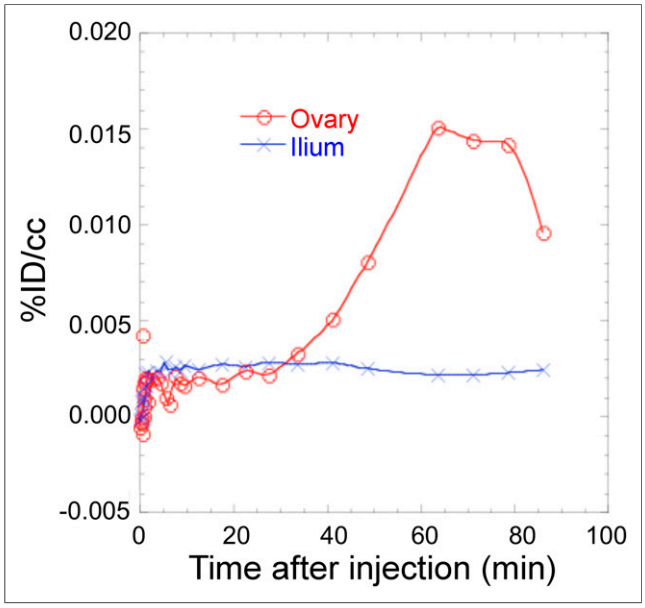

FIGURE 3. Time–activity curve of ^{11}C-vorozole in midcycle ovary. Figure depicts tracer uptake in right ovary of young woman on day 14 of her menstrual cycle (counting from first day of menstrual flow) according to self-report. Cycle phase was verified by high levels of estrogen and luteinizing hormone and low levels of progesterone found in plasma on day of scan. Time–activity curve of ilium from same scan is shown for comparison. %ID = percentage injected dose.

The highest SUVs in the human body were recorded from liver, followed by brain in men and ovary in women (Table 1; Figs. 2 and 3). Thus, mean brain SUVs in men (2.6 ± 0.12 in thalamus) were higher than SUVs in other organs in the male body (ranging from 0.48 ± 0.05 in lungs to 1.5 ± 0.13 in kidneys). In women, mean ovarian SUVs (3.08 ± 0.7) were comparable to brain levels and higher than other organs in the female body. In shared organs, there was a small but significant difference in aromatase SUVs, with values higher in men than in women (Table 1).

SUVs showed good reproducibility across organs and brain regions, such that baseline and retest values were mostly very close and statistically indistinguishable (P = 0.9, Fig. 4). Uptake was significantly reduced by pretreatment with letrozole in high-uptake brain regions but not in the liver. Peripheral organs with low uptake did not show a significant effect of blocking.

Individual plasma testosterone and estrogen levels were within the established norms for adult men and women, with testosterone levels of 250–570 ng/mL in men and less than 20–32 ng/mL in women and estrogen levels of less than 50–114 pg/mL in men and 84–250 pg/mL in premenopausal women. There was no correlation between estrogen, testosterone, or the estrogen-to-testosterone ratio and SUV in the various organs in men and postmenopausal women. In premenopausal women, ovarian SUVs near the time of ovulation (midcycle, 5.0 ± 1) were significantly higher ($P < 0.05$, 1-way ANOVA followed by the Fisher protected least significant

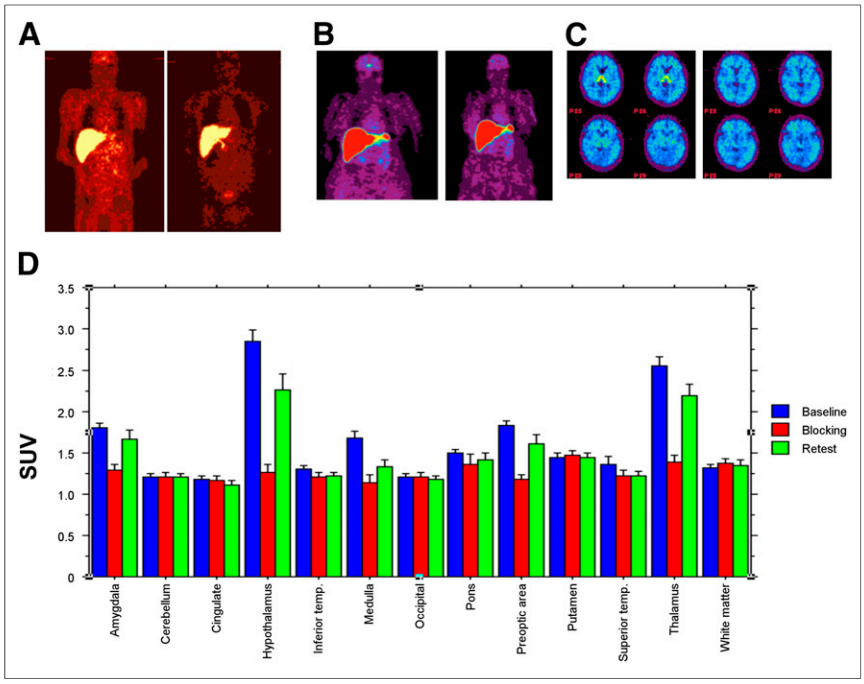

FIGURE 4. Specificity and reproducibility of ^{11}C-vorozole uptake in men and women. (A and B) Representative images showing global effect of blocking in all organs besides liver. (A) Semiquantitative whole-body images from man, with baseline scan on left and blocking on right. (B) Body scans of postmenopausal woman, with baseline scan on left and blocking on right. (C) Baseline (left) and blocked (right) axial brain images at level of pulvinar nucleus of thalamus. (D) Brain SUV analysis: bars represent mean ± SEM of regional SUVs under baseline, blocking, and retest conditions. Two-way ANOVA by treatment (baseline, blocking, retest) and region revealed highly significant effects ($P < 0.0001$) of treatment and ROI as well as highly significant ($P < 0.0001$) region × treatment interaction. Subsequent post hoc comparison showed that blocked SUVs were significantly different from baseline and retest ($P < 0.0001$), which were not different from each other ($P = 0.23$).

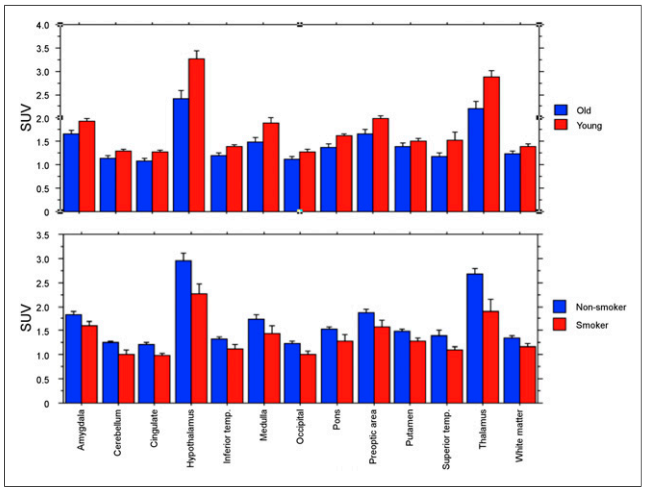

FIGURE 5. Effects of age (top) and cigarette smoking (bottom) on brain uptake of ^{11}C-vorozole. Bars represent mean ± SEM of regional SUV in 4–20 subjects per region. Two-way ANOVA revealed highly significant effects of age ($F_1 = 75.3$, $P < 0.0001$) and region ($F_{12} = 65$, $P < 0.0001$) as well as significant age × ROI interaction ($F_{12} = 2.7$, $P = 0.0017$). Four active smokers were compared with 24 age- and sex-matched nonsmokers. Two-way ANOVA revealed significant effects of smoking ($F_1 = 25.2$, $P < 0.0001$) and region ($F_{12} = 22.45$, $P < 0.0001$) and nonsignificant smoking × region interaction ($P = 0.74$). Nicotine levels in 4 active smokers ranged from 0 to 22 μg/mL (mean, 9.2 μg/mL) and cotinine levels ranged from 29 to 460 μg/mL (mean, 189 μg/mL). Two occasional smokers (by self-report) who did not have measureable levels of nicotine or cotinine in plasma on day of scan were not included in analysis. Old = age > 50 y; young = age ≤ 50 y.

difference) than those measured in the late luteal (1.5 ± 0.2) or early follicular (1.3 ± 0.05) phase as determined from self-report and confirmed by hormone levels.

Separate analysis of brain SUVs revealed significantly lower brain uptake in subjects over age 50 y and active cigarette smokers (Fig. 5). However, these factors did not influence the rank order of tracer distribution in the brain (*4,23*), and the effects were considerably smaller than those seen with clinical doses of letrozole (blocking study).

Urine samples obtained and counted at the end of the PET acquisition (20 samples, 115–575 mL) were included in the dosimetry estimation model. Total body dosimetry was 3.2 μSv/MBq (11.90 mrem/mCi). All doses injected were below 296 MBq, so the maximum absorbed dose was 95.20 mrem (25.7 μSv) per ^{11}C-vorozole scan (Table 2). The dose-limiting organ was the ovary in young women at midcycle, whereas the liver was the dose-limiting organ in all other groups and endocrine states.

DISCUSSION

The results of the studies reported here suggest that ^{11}C-vorozole is a useful radiotracer for the noninvasive assessment of aromatase availability in healthy human subjects. Our results provide baseline information for future studies in neuropsychiatric disorders and cancer (*24,25*). We show that ^{11}C-vorozole is taken up by all major organs in humans, as would be expected on the basis of the reportedly widespread expression of Cyp19A1 in human organs, systems, and cell types, controlled by a large number of tissue-specific promoters (*26*).

Tracer uptake was low in most peripheral organs, including lung, muscle, bone, and male and female breasts and reproductive organs. The 2 exceptions were the liver and ovaries. Liver uptake was high, but the fact that this uptake was not blocked by letrozole pretreatment suggests that liver radioactivity is not associated with aromatase but rather reflects the presence of labeled metabolites or binding to other enzymes abundant in the liver.

Mean ovarian uptake was also high though strongly dependent on hormonal status and menstrual cycle phase, with peak values around midcycle averaging more than 3 times the values in the early follicular or late luteal phase in young women. The increased uptake appears to be associated with ovulation rather than circulating hormone levels since it consistently occurred in 1 ovary (1 side) only. This observation resonates with unilateral increases in glucose metabolism (^{18}F-FDG uptake) observed in previous PET studies of the ovaries in healthy women (*27,28*) and suggests that the use of ^{11}C-vorozole for ovarian cancer diagnosis and subtyping in young women should be performed in the early follicular or late luteal stage, with no restriction in postmenopausal women (*27*). The high sensitivity of PET coupled with the specificity of ^{11}C-vorozole offers the potential of early diagnosis and identification of the subset of ovarian tumors that overexpresses aromatase and is likely to respond to aromatase inhibitors, estimated as

TABLE 2
Radiation Exposure (Dosimetry) Associated with ^{11}C-Vorozole PET

Organ	mRem/37 MBq	mRem/196-MBq dose)	μSv/MBq	μSv/296 MBq
Adrenals	13.80	110.40	3.7	29.8
Brain	18.30	146.40	4.9	39.5
Breasts	52.20	417.60	14.1	112.8
Gallbladder	16.80	134.40	4.5	36.3
Lower large intestine	11.00	88.00	3.0	23.8
Small intestine	11.90	95.20	3.2	25.7
Stomach	11.60	92.80	3.1	25.1
Upper large intestine	12.20	97.60	3.3	26.4
Heart	17.00	136.00	4.6	36.7
Kidneys	22.30	178.40	6.06	48.2
Liver	57.40	459.20	15.5	124.0
Lungs	11.20	89.60	3.0	24.2
Muscle	9.78	78.24	2.6	21.1
Ovaries (young, ovulating)	312.00	2,496.00	84.2	673.9
Ovaries (nonovulating)	10.03	80.24	2.7	21.7
Pancreas	13.90	111.20	3.9	30.0
Red marrow	9.34	74.72	2.5	20.2
Osteogenic	14.10	112.80	3.8	30.5
Skin	8.04	64.32	2.2	17.4
Spleen	22.50	180.00	6.1	48.6
Testes	7.14	57.12	1.9	15.4
Thymus	10.40	83.20	2.8	22.5
Thyroid	9.70	77.60	2.6	21.0
Urinary bladder	10.70	85.60	2.9	23.1
Uterus	13.40	107.20	3.6	28.9
Total body	11.90	95.20	3.2	25.7

33%–80% of ovarian tumors (*25*). Further studies of ^{11}C-vorozole uptake in the premenopausal ovary may establish a role for aromatase imaging in the diagnosis and treatment management of other endocrine reproductive disorders.

The highly conserved brain regional distribution pattern of aromatase in young and old men and women reported here, showing highest tracer uptake in thalamus, replicates and extends our published results from a smaller group of young individuals (*4,5,23*). We also show that brain uptake is significantly blocked by pretreatment with a pharmacologic dose of letrozole, whereas regional SUVs in individual subjects are similar when scanning is repeated after a 2- to 6-wk interval.

In the current study, the first to compare brain, torso, and pelvis in a relatively large group of the same subjects, we also made the rather surprising observation that the brain of men has the highest estrogen synthesizing capacity in the male body and that the only peripheral organ with similar capacity is the female ovary during ovulation. However, unlike ovarian uptake, regional brain uptake of ^{11}C-vorozole did not vary across the menstrual cycle in premenopausal women. These results echo rodent studies showing that brain aromatase is not significantly regulated by the estrous cycle in rodents (*6*), although we did observe significant menstrual cycle–dependent changes in modeled kinetic parameters in female baboon brain (*29*). Other factors, including age, sex, and cigarette smoking, had significant effects on brain SUVs. Thus, small but consistent sex differences in SUV were detected in the brain, with higher values in all men relative to all women. Previous studies on postmortem brain samples (*24,30–32*) reported similar levels of brain aromatase activity and gene expression in men and women. Conversely, results from animal studies demonstrated higher levels of brain aromatase in males and suggested that testosterone was a positive modulator of aromatase in the hypothalamic-preoptic area (*6,7*). The discrepancy most likely reflects issues of statistical power because previous human studies, including our published pilot (*4*), included fewer subjects.

Normal aging and postmenopausal status were associated with decreased SUV throughout the brain in both men and women, although the size of the effect was region-dependent, with larger age-related decreases in the thalamus and paraventricular hypothalamus than in the basal ganglia.

Finally, cigarette smokers had significantly lower ^{11}C-vorozole SUVs throughout the brain than did nonsmoking controls, similar to the effect of nicotine on brain aromatase in baboons (*33*).

Taken together, these findings support the notion that aromatase expression is regulated in a species-, sex-, organ-, and brain region–specific manner. Such specific regulation may be the result of tissue-specific aromatase promoters, which were identified in

animal and human tissues (*26,34*). Since other promoters besides the brain-specific exon 1.f (*30*) are expressed in the human brain, this heterogeneity may provide the basis for brain region–specific regulation of aromatase in humans, which may be exploited in the future to design organ- and region-specific interventions.

CONCLUSION

^{11}C-vorozole PET is useful in measuring aromatase expression in the human body, supporting future investigation as a tool for diagnosis, treatment monitoring, and treatment optimization, as well as pharmacokinetic and pharmacodynamic assessment of new aromatase inhibitors in development for cancer and other disorders (*35*) in which aromatase inhibition is indicated.

DISCLOSURE

The costs of publication of this article were defrayed in part by the payment of page charges. Therefore, and solely to indicate this fact, this article is hereby marked "advertisement" in accordance with 18 USC section 1734. This study was performed at Brookhaven National Laboratory using the infrastructure support of the U.S. Department of Energy OBER (DE-AC02-98CH10886). The study was supported in part by NIH grants K05DA020001 and 1R21EB012707 and by the National Institute of Alcohol Abuse and Alcoholism. No other potential conflict of interest relevant to this article was reported.

ACKNOWLEDGMENTS

We thank Michael Schueller, Donald Warner, Barbara Hubbard, Pauline Carter, Millard Jayne, Colleen Shea, Youwen Xu, Lisa Muench, and Karen Apelskog-Torres for their assistance, and we thank the people who volunteered for this study.

REFERENCES

1. Danielson PB. The cytochrome P450 superfamily: biochemistry, evolution and drug metabolism in humans. *Curr Drug Metab.* 2002;3:561–597.
2. Simpson ER, Clyne C, Rubin G, et al. Aromatase: a brief overview. *Annu Rev Physiol.* 2002;64:93–127.
3. Roselli CE, Resko JA. Cytochrome P450 aromatase (CYP19) in the non-human primate brain: distribution, regulation, and functional significance. *J Steroid Biochem Mol Biol.* 2001;79:247–253.
4. Biegon A, Kim S-W, Alexoff DL, et al. Unique distribution of aromatase in the human brain: in vivo studies with PET and [N-methyl-^{11}C]vorozole. *Synapse.* 2010;64:801–807.
5. Biegon A, Fowler JS, Kim S-W, Logan J, Pareto D, Wang G-J. Distribution of aromatase in the human brain. In: Balthazart J, Ball JF, eds. *Brain Aromatase, Estrogens and Behavior.* New York, NY: Oxford University Press; 2012:89–99.
6. Roselli CE, Ellinwood WE, Resko JA. Regulation of brain aromatase activity in rats. *Endocrinology.* 1984;114:192–200.
7. Abdelgadir SE, Resko JA, Ojeda SR, Lephart ED, McPhaul MJ, Roselli CE. Androgens regulate aromatase cytochrome P450 messenger ribonucleic acid in rat brain. *Endocrinology.* 1994;135:395–401.
8. Garcia-Segura LM. Aromatase in the brain: not just for reproduction anymore. *J Neuroendocrinol.* 2008;20:705–712.
9. Saldanha CJ, Duncan KA, Walters BJ. Neuroprotective actions of brain aromatase. *Front Neuroendocrinol.* 2009;30:106–118.
10. Bulun SE, Simpson ER. Aromatase expression in women's cancers. *Adv Exp Med Biol.* 2008;630:112–132.
11. Fedele L, Somigliana E, Frontino G, Benaglia L, Vigano P. New drugs in development for the treatment of endometriosis. *Expert Opin Investig Drugs.* 2008;17:1187–1202.
12. Márquez-Garbán DC, Chen HW, Goodglick L, Fishbein MC, Pietras RJ. Targeting aromatase and estrogen signaling in human non-small cell lung cancer. *Ann N Y Acad Sci.* 2009;1155:194–205.
13. Miceli V, Cervello M, Azzolina A, Montalto G, Calabrò M, Carruba G. Aromatase and amphiregulin are correspondingly expressed in human liver cancer cells. *Ann N Y Acad Sci.* 2009;1155:252–256.
14. Vanden Bossche H, Willemsens G, Roels I, et al. R76713 and enantiomers: selective nonsteroidal inhibitors of the cytochrome P450-dependent oestrogen synthesis. *Biochem Pharmacol.* 1990;40:1707–1718.
15. Cohen MH, Johnson JR, Li N, Chen G, Pazdur R. Approval summary: letrozole in the treatment of postmenopausal women with advanced breast cancer. *Clin Cancer Res.* 2002;8:665–669.
16. Lidström P, Bonasera TA, Kirilovas D, et al. Synthesis, in vivo rhesus monkey biodistribution and in vitro evaluation of a ^{11}C-labelled potent aromatase inhibitor: [N-methyl-^{11}C]vorozole. *Nucl Med Biol.* 1998;25:497–501.
17. Takahashi K, Bergström M, Frändberg P, Vesström E-L, Watanabe Y, Långström B. Imaging of aromatase distribution in rat and rhesus monkey brains with ^{11}C-vorozole. *Nucl Med Biol.* 2006;33:599–605.
18. Kil KE, Biegon A, Ding YS, et al. Synthesis and PET studies of [^{11}C-cyano] letrozole (Femara), an aromatase inhibitor drug. *Nucl Med Biol.* 2009;36:215–223.
19. Kim SW, Biegon A, Katsamanis Z, et al. Reinvestigation of the synthesis and evaluation of [N-methyl-^{11}C]vorozole, a radiotracer targeting cytochrome P450 aromatase. *Nucl Med Biol.* 2009;36:323–334.
20. Takahashi K, Hosoya T, Onoe K, et al. ^{11}C-cetrozole: an improved C-^{11}C-methylated PET probe for aromatase imaging in the brain. *J Nucl Med.* 2014;55:852–857.
21. Alexoff DL, Shea C, Wolf AP, et al. Plasma input function determination for PET using a commercial laboratory robot. *Nucl Med Biol.* 1995;22:893–904.
22. Stabin MG, Sparks RB, Crowe E. OLINDA/EXM: the second-generation personal computer software for internal dose assessment in nuclear medicine. *J Nucl Med.* 2005;46:1023–1027.
23. Logan J, Kim SW, Pareto D, et al. Kinetic analysis of ^{11}C-vorozole binding in the human brain with PET. *Mol Imaging.* 2014;13:1–12.
24. Hiltunen M, Iivonen S, Soininen H. Aromatase enzyme and Alzheimer's disease. *Minerva Endocrinol.* 2006;31:61–73.
25. Li YF, Hu W, Fu SQ, Li JD, Liu JH, Kavanagh JJ. Aromatase inhibitors in ovarian cancer: is there a role? *Int J Gynecol Cancer.* 2008;18:600–614.
26. Bulun SE, Sebastian S, Takayama K, Suzuki T, Sasano H, Shozu M. The human CYP19 (aromatase P450) gene: update on physiologic roles and genomic organization of promoters. *J Steroid Biochem Mol Biol.* 2003;86:219–224.
27. Lerman H, Metser U, Grisaru D, Fishman A, Kievshitz G, Even-Sapir E. Normal and abnormal ^{18}F-FDG endometrial and ovarian uptake in pre- and post-menopausal patients: assessment by PET/CT. *J Nucl Med.* 2004;45:266–271.
28. Nishizawa S, Inubushi M, Okada H. Physiological ^{18}F-FDG uptake in the ovaries and uterus of healthy female volunteers. *Eur J Nucl Med Mol Imaging.* 2005;32:549–556.
29. Pareto D, Biegon A, Alexoff D, et al. In vivo imaging of brain aromatase in female baboons: [^{11}C]orozole kinetics and effect of menstrual cycle. *Mol Imaging.* 2013;12:518–524.
30. Sasano H, Takahashi K, Satoh F, Nagura H, Harada N. Aromatase in the human central nervous system. *Clin Endocrinol (Oxf).* 1998;48:325–329.
31. Steckelbroeck S, Heidrich DD, Stoffel-Wagner B, et al. Characterization of aromatase cytochrome P450 activity in the human temporal lobe. *J Clin Endocrinol Metab.* 1999;84:2795–2801.
32. Stoffel-Wagner B, Watzka M, Schramm J, Bidlingmaier F, Klingmüller D. Expression of CYP19 (aromatase) mRNA in different areas of the human brain. *J Steroid Biochem Mol Biol.* 1999;70:237–241.
33. Biegon A, Kim S-W, Logan J, Hooker JM, Muench L, Fowler JS. Nicotine blocks brain estrogen synthase (aromatase): in vivo PET studies in female baboons. *Biol Psychiatry.* 2010;67:774–777.
34. Golovine K, Schwerin M, Vanselow J. Three different promoters control expression of the aromatase cytochrome p450 gene (cyp19) in mouse gonads and brain. *Biol Reprod.* 2003;68:978–984.
35. Legro RS, Brzyski RG, Diamond MP, et al. NICHD Reproductive Medicine Network. Letrozole versus clomiphene for infertility in the polycystic ovary syndrome. *N Engl J Med.* 2014;371:119–129.